

Electronic Supplementary Information

Peri-Anthracenethioindigo: a Scaffold for Efficient All-Red-Light and NIR Molecular Photoswitching

Laura Köttner,[§] Elias Ciekalski,[§] Henry Dube^{§*}

[§] Friedrich-Alexander-Universität Erlangen-Nürnberg, Department of Chemistry and Pharmacy, Nikolaus-Fiebiger-Str. 10, 91058 Erlangen, Germany.

Table of Content

Materials and general methods.....	2
Synthesis of PAT 1	4
9-Bromo-10-iodoanthracene (2).....	5
Methyl 2-((10-bromoanthracen-9-yl)thio)acetate (3)	6
Methyl 2-((10-mesitylanthracen-9-yl)thio)acetate (4)	7
2-((10-Mesitylanthracen-9-yl)thio)acetic acid (5).....	8
7-Mesityldibenzo[<i>de,h</i>]thiochromen-3(2 <i>H</i>)-one (6).....	9
Peri-anthracenethioindigo (PAT 1).....	10
Thermal isomerization.....	11
Photophysical and photochemical properties	17
PSS determination using ¹ H NMR spectroscopy	17
PSS determination using UV/Vis spectroscopy.....	19
Photoisomerization followed by UV/Vis spectroscopy.....	20
Molar absorption coefficients.....	22
Quantum Yield Determination	24
Photostability	28
Incorporation into Polymer and Photoswitching.....	30
NMR spectra	31
References.....	37

Materials and general methods

Unless stated otherwise, all experiments were conducted under atmospheric conditions. When using anhydrous solvents, reactions were carried out under argon atmosphere to maintain anhydrous conditions. Schlenk flasks used for this purpose were purged three times with argon. Syringes and needles used for reagent and solvent dosing were flushed three times with argon. Solvents were degassed by bubbling through argon for 10 minutes, thus saturating the solvents with argon.

Reagents and solvents were obtained from *BLDpharm*, *Fisher Scientific*, *Sigma-Aldrich*, or *TCI* in the qualities *puriss.*, *p.a.*, or *purum* and used as received. Reactions were monitored on *Merck Silica 60 F254* TLC plates and detection was done by irradiation with UV light (254 nm or 366 nm).

Column chromatography was performed with silica gel 60 (Merck, particle size 0.063- 0.200 mm) and distilled technical solvents.

^1H NMR and ^{13}C NMR spectra were measured on a *Bruker Avance NEO HD 400 MHz*, *BrukerAvance Neo HDX 500 MHz*, or *Bruker Avance Neo HDX 600 MHz* NMR spectrometer. Deuterated solvents were obtained from *Deutero GmbH* or *Sigma-Aldrich* and used without further purification. The chemical shifts are given in parts per million (ppm) on the delta scale (δ) relative to tetramethylsilane as external standard. Residual solvent signals in the ^1H and ^{13}C NMR spectra were used as internal reference. The following solvents were used with their internal reference: benzene- d_6 : $\delta_{\text{H}} = 7.16$ ppm, $\delta_{\text{C}} = 128.06$ ppm; chloroform- d_1 : $\delta_{\text{H}} = 7.26$ ppm, $\delta_{\text{C}} = 77.16$ ppm; dichloromethane- d_2 : $\delta_{\text{H}} = 5.32$ ppm; tetrahydrofuran- d_8 : $\delta_{\text{H}} = 3.58$ ppm. The resonance multiplicity is indicated as *s* (singlet), *d* (doublet), *t* (triplet), *m* (multiplet). The coupling constant values (*J*) are given in hertz (Hz). Signal assignments are given in the experimental part with the arbitrary numbering indicated.

Atmospheric pressure photoionization (APPI) mass spectra were measured on a *MicroTOF II* spectrometer. The found masses from *high resolution* measurements (HR-APPI-MS) are reported in *m/z* units with *M* as the molecular ion.

Melting points (m.p.) were determined on a *Büchi B-540* melting point apparatus in open capillaries.

Infrared spectra were measured on a *Perkin Elmer Spectrum BX-FT-IR* spectrometer equipped with a *Smith DuraSample IR II ATR*-device and a *Varian 660-IR ATR* mode.

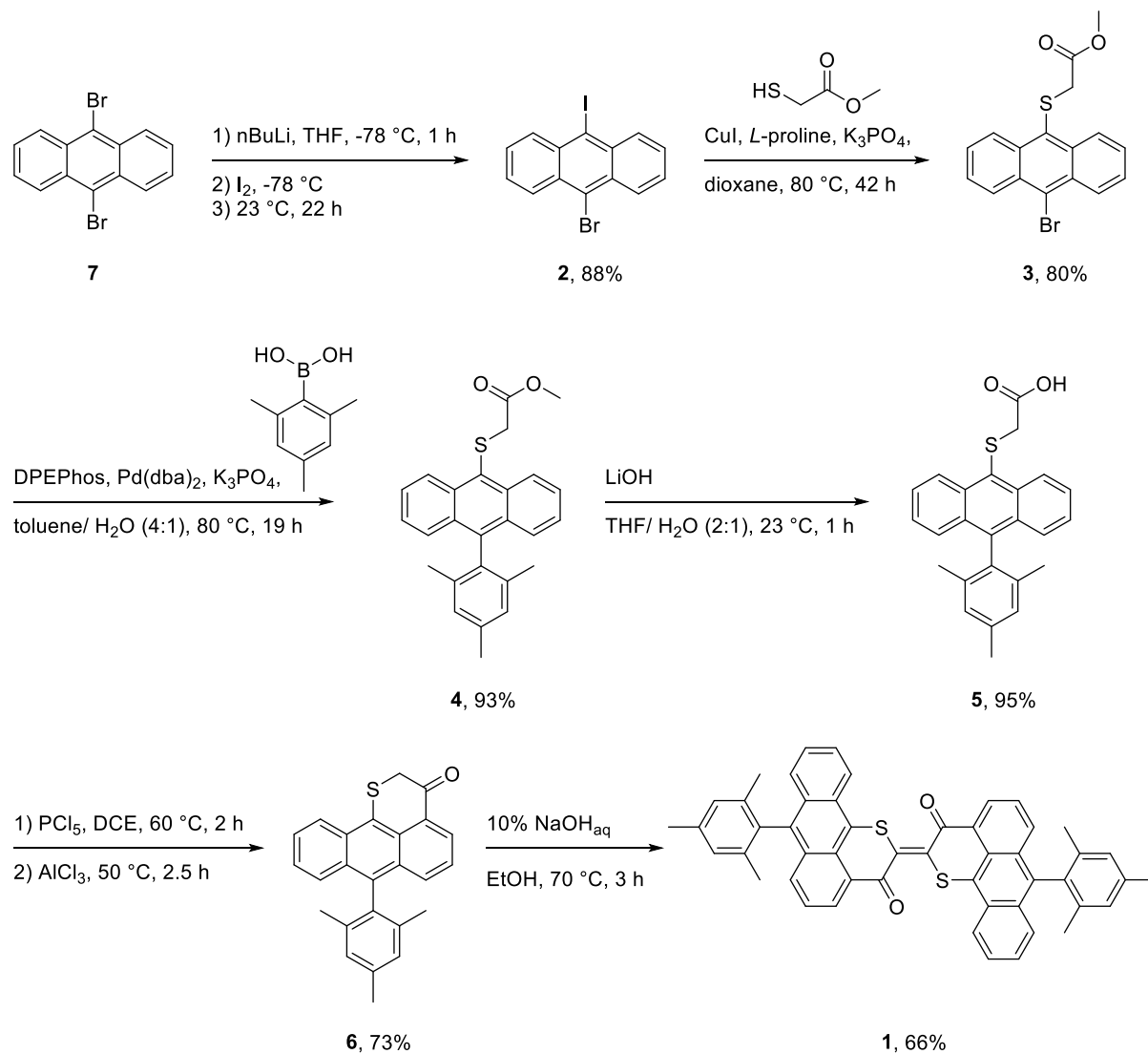
Transmittance values are described by wavenumber (cm^{-1}) as strong (*s*), medium (*m*) and weak (*w*).

UV/Vis spectra were recorded on a *Varian Cary 60* spectrophotometer with a quartz cuvette (10 mm). Spectral grade solvents were obtained from *VWR* and *Merck*. Absorption wavelengths (λ) are given in nm and the molar absorption coefficients (ϵ) in $\text{L}\cdot\text{mol}^{-1}\cdot\text{cm}^{-1}$. For heating experiments a *Varian Cary Single cell Peltier Accessory* was used.

Photoisomerization experiments were conducted using LEDs from *Roithner Lasertechnik GmbH* and *Thorlabs Inc.* (550 nm, 590 nm, 617 nm, 619 nm, 720 nm, 730 nm, 780 nm) for illumination at 23 °C.

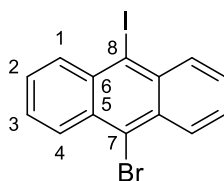
Synthesis of PAT 1

PAT 1 was synthesized in a 6-step synthesis starting from commercially available 9,10-dibromoanthracene (Scheme S1). The first step follows a published procedure.^[1]



Scheme S1 Synthesis route to access PAT 1 with an overall yield of 30%.

9-Bromo-10-iodoanthracene (**2**)



9,10-Dibromoanthracene (3.36 mg, 10 mmol, 1.0 equiv.) was suspended in dry THF (50 mL) and the mixture was purged with argon. A hexane solution of *n*-butyllithium (4.80 mL, 12 mmol, 1.2 equiv.) was added dropwise to the solution at $-78\text{ }^{\circ}\text{C}$. The reaction mixture was stirred at this temperature for 1 h. A THF solution (10 mL) of iodine (3.05 mg, 12 mmol, 1.2 equiv.) was added dropwise to the flask at $-78\text{ }^{\circ}\text{C}$ and the mixture was stirred for 1 h at that temperature and then warmed to $23\text{ }^{\circ}\text{C}$. After stirring for 22 h at $23\text{ }^{\circ}\text{C}$, the reaction was quenched with an aqueous solution of NaHSO_3 . The desired precipitate was filtered and collected and the remaining filtrate was again diluted with NaHSO_3 and the solid filtered and collected. The obtained crude product was washed with H_2O and cold methanol to afford **2** (3.35 g, 8.76 mmol, 88%) as a yellow solid.

$^1\text{H NMR}$ (400 MHz, CDCl_3) δ (ppm) = 8.57 (m, 4H), 7.63 (m, 4H).

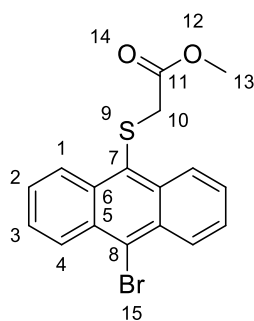
$^{13}\text{C NMR}$ (101 MHz, CDCl_3) δ (ppm) = 134.38, 134.22, 131.09, 128.71, 128.11, 127.63, 125.65, 106.57.

HRMS (APPI), $[\text{MH}]^+$: m/z calc.: 382.8927 for $[\text{C}_{14}\text{H}_9\text{BrI}]^+$, found: 382.8927.

m. p.: 219 – 221 $^{\circ}\text{C}$.

IR: $\tilde{\nu}$ (cm^{-1}) = 1618.7 (*w*), 1434.4 (*m*), 1298.0 (*m*), 1249.1 (*m*), 1147.1 (*w*), 1029.0 (*w*), 917.2 (*s*), 841.1 (*w*), 745.4 (*s*), 667.8 (*w*), 604.8 (*m*), 571.2 (*m*).

Methyl 2-((10-bromoanthracen-9-yl)thio)acetate (**3**)



2 (2.00 g, 5.22 mmol, 1.0 equiv.), CuI (149 mg, 0.78 mmol, 0.15 equiv.), *L*-proline (120 mg, 1.04 mmol, 0.20 equiv.), and K₃PO₄ (12.22 g, 10.4 mmol, 2.0 equiv.) were added to a Schlenk flask, which was evacuated and flushed with argon three times. Thioglycolic acetate (560 μ L, 6.27 mmol, 1.2 equiv.) and dry dioxane (100 mL) were added, purged with argon and stirred at 80 °C for 41 h. After the reaction mixture was cooled to 23 °C, brine (250 mL) was added and the product was extracted with CH₂Cl₂ (3 x 150 mL). The combined organic phases were concentrated *in vacuo* and the crude product was purified by column chromatography (SiO₂, *i*-hex : EtOAc 95 :5) to afford **3** as a light yellow solid (1.51 g, 4.19 mmol, 80%).

¹H NMR (400 MHz, CDCl₃) δ (ppm) = 9.04 – 8.91 (m, 2H, H-C(1)), 8.67 – 8.52 (m, 2H, H-C(4)), 7.71 – 7.55 (m, 4H, H-C(2), H-C(3)), 3.53 (s, 2H, H₂-C(10)), 3.38 (s, 3H, H₃-C(13)).

¹³C NMR (101 MHz, CDCl₃) δ (ppm) = 170.0 (C(11)), 135.2 (C(6)), 131.0 (C(5)), 128.8 (C(4)), 128.5 (C(7)), 127.4 (C(2), C(3)), 127.2 (C(1)), 127.1, (C(8)), 52.3 (C(13)), 38.3 (10)).

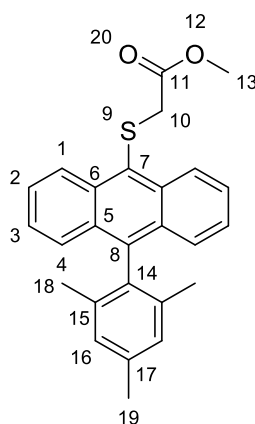
R_f = 0.35 (SiO₂, *i*-hex : EtOAc 9:1).

HRMS (APPI), [MH]⁺: *m/z* calc.: 360.9892 for [C₁₇H₁₄BrO₂S]⁺, found: 360.9894.

m. p.: 79 – 80 °C.

IR: $\tilde{\nu}$ (cm⁻¹) = 3203.2 (*m*), 1727.2 (*m*), 1610.1 (*w*), 1431.0 (*s*), 1340.6 (*m*), 1193.6 (*m*), 1099.3 (*m*), 1013.1 (*m*), 801.0 (*w*), 749.4 (*s*), 651.1 (*m*), 607.0 (*w*), 543.9 (*m*), 426.3 (*w*).

Methyl 2-((10-mesitylanthracen-9-yl)thio)acetate (**4**)



3 (434 mg, 1.2 mmol, 1.0 equiv.), 2,4,6-trimethylphenylboronic acid (262 mg, 1.6 mmol, 1.3 equiv.), K_3PO_4 (764 mg, 3.6 mmol, 3.0 equiv.), DPEPhos (129 mg, 0.24 mmol, 0.20 equiv.), and $Pd(dba)_2$ (104 mg, 0.18 mmol, 0.15 equiv.) were added to a Schlenk flask, which was evacuated and flushed with argon three times. Then toluene (14.4 mL) and H_2O (3.6 mL) were added and the mixture was purged with argon. The reaction mixture was heated at 80 °C for 19 h. After the reaction mixture was cooled to 23 °C and poured into water (100 mL), the organic phase was separated, and the aqueous phase was extracted with CH_2Cl_2 (3 x 100mL). The organic extracts were combined, dried over anhydrous Na_2SO_4 , and concentrated *in vacuo*. The product **4** was purified by column chromatography (SiO_2 , *i*-hex : EtOAc 95 : 5) and isolated as a light yellow oil (445 mg, 1.1 mmol, 93%).

1H NMR (600 MHz, $CDCl_3$) δ (ppm) = 9.01 (dt, J = 8.9, 1.0 Hz, 2H, H-C(1)), 7.60 (ddd, J = 8.9, 6.4, 1.3 Hz, 2H, H-C(2)), 7.52 (dt, J = 8.7, 1.1 Hz, 2H, H-C(4)), 7.36 (ddd, J = 8.7, 6.4, 1.2 Hz, 2H, H-C(3)), 7.09 (s, 1H, H-C(16)), 3.59 (s, 2H, H_2 -C(10)), 3.33 (s, 3H, H_3 -C(13)), 2.46 (s, 3H, H_3 -C(19)), 1.69 (s, 6H, H_3 -C(19)).

^{13}C NMR (101 MHz, $CDCl_3$) δ (ppm) = 170.3 (C(11)), 139.5 (C(8)), 137.6 (C(17)), 137.4 (C(15)), 134.7 (C(16)), 134.4 (C(14)), 130.3 (C(5)), 128.5 (C(16)), 127.1 (C(1)), 127.0 (C(2)), 126.9 (C(4)), 125.8 (C(3)), 52.1 (C(13)), 38.2 (C(10)), 21.4 (C(19)), 20.0 (C(18)).

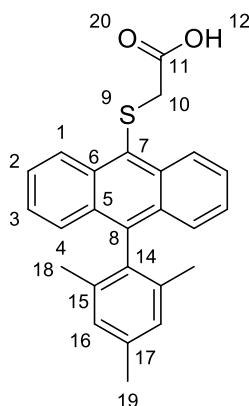
R_f = 0.48 (SiO_2 , *i*-hex : EtOAc 9:1).

HRMS (APPI), $[MH]^+$: m/z calc.: 401.1570 for $[C_{26}H_{25}O_2S]^+$, found: 401.1571.

Decomposition: 178 – 182 °C.

IR: $\tilde{\nu}$ (cm^{-1}) = 2954.6 (*w*), 1724.8 (*m*), 1649.1 (*w*), 1589.6 (*w*), 1437.2 (*w*), 1409.2 (*w*), 1285.9 (*m*), 1261.0 (*m*), 1193.1 (*w*), 1132.0 (*m*), 1094.8 (*w*), 1016.5 (*s*), 982.1 (*m*), 942.9 (*w*), 927.7 (*w*), 877.3 (*w*), 797.9 (*m*), 755.4 (*s*), 693.1 (*s*), 603.7 (*s*), 580.1 (*m*), 558.0 (*w*), 527.9 (*w*), 545.6 (*m*), 478.6 (*m*), 431.9 (*w*), 403.4 (*m*).

2-((10-Mesitylanthracen-9-yl)thio)acetic acid (**5**)



4 (445 mg, 1.1 mmol, 1.0 equiv.) was dissolved in THF (12 mL) and H₂O (6 mL). LiOH (53.0 mg, 2.2 mmol, 2.0 equiv.) was added and the mixture was stirred at 23 °C for 1 h. The reaction was quenched by addition of an aqueous solution of NH₄Cl (200 mL). The product was extracted with EtOAc (3 x 150 mL), the organic phases were combined, washed with brine (100 mL), dried over Na₂SO₄ and the solvent was removed *in vacuo*. The product **5** was isolated without further purification as a yellow solid (402 mg, 1.0 mmol, 95%).

¹H NMR (400 MHz, CDCl₃) δ (ppm) = 9.01 (dt, J = 8.9, 1.0 Hz, 2H, H-C(1)), 7.58 (ddd, J = 8.9, 6.4, 1.3 Hz, 2H, H-C(2)), 7.51 (dt, J = 8.7, 1.0 Hz, 2H, H-C(4)), 7.35 (ddd, J = 8.7, 6.4, 1.2 Hz, 2H, H-C(3)), 7.08 (s, 2H, H-C(16)), 3.61 (s, 2H, H₂-C(10)), 2.45 (s, 3H, H₃-C(19)), 1.68 (s, 6H, H₃-C(18)).

¹³C NMR (101 MHz, CDCl₃) δ (ppm) = 174.7 (C(11)), 139.7 (C(8)), 137.6 (C(17)), 137.5 (C(15)), 134.6 (C(6)), 134.4 (C(14)), 130.3 (C(5)), 128.5 (C(16)), 127.1 (C(2)), 127.0 (C(1)), C(4)), 126.5(C(7)), 125.8 (C(3)), 38.2 (C(10)), 21.4 (C(19)), 20.1 (C(18)).

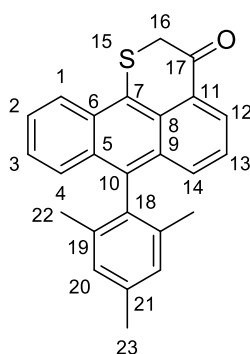
R_f = 0.51 (SiO₂, *i*-hex : EtOAc 7:3 + 1% HOAc).

HRMS (APPI), [MH]⁺: m/z calc.: 409.1233 for [C₂₅H₂₂NaO₂S]⁺, found: 409.1225.

m. p.: 181 – 182 °C.

IR: $\tilde{\nu}$ (cm⁻¹) = 2917.6 (*m*), 2851.0 (*w*), 1698.2 (*s*), 1433.6 (*m*), 1297.4 (*w*), 1259.1 (*w*), 11.29.2 (*w*), 1020.4 (*m*), 943.7 (*w*), 851.2 (*w*), 794.6 (*w*), 765.3 (*s*), 698.0 (*w*), 680.9 (*m*), 662.6 (*m*), 617.4 (*m*), 467.1 (*w*).

7-Mesityldibenzo[de,h]thiochromen-3(2H)-one (6)



5 (38 mg, 0.1 mmol, 1.0 equiv.) was dissolved in DCE (5 mL) and PCl_5 (31 mg, 0.15 mmol, 1.5 equiv.) was added. The reaction mixture was stirred at 60 °C for 2 h. AlCl_3 (20 mg, 0.15 mmol, 1.5 equiv.) was added at 50 °C and the mixture was stirred for another 2.5 h at that temperature. The reaction was quenched by the addition of 2 M aqueous HCl (50 mL) and the product was extracted with CH_2Cl_2 (3 x 50 mL). The organic phases were combined, dried over Na_2SO_4 and the solvent was removed *in vacuo*. Product **6** was isolated without further purification as a yellow solid (27 mg, 0.073mmol, 73%).

$^1\text{H NMR}$ (400 MHz, CDCl_3) δ (ppm) = 8.51 (d, J = 8.8 Hz, 1H, H-C(1)), 8.27 (dd, J = 7.0, 1.2 Hz, 1H, H-C(12)), 7.80 (dd, J = 8.7, 1.3 Hz, 1H, H-C(14)), 7.60 (ddd, J = 9.0, 6.5, 1.2 Hz, 1H, H-C(2)), 7.51 (d, J = 8.7 Hz, 1H, H-C(4)), 7.47 – 7.37 (m, 2H, H-C(3, 13)), 7.09 (s, 2H, H-C(20)), 3.98 (s, 2H, $\text{H}_2\text{-C}(16)$), 2.46 (s, 3H, $\text{H}_3\text{-C}(23)$), 1.70 (s, 6H, $\text{H}_3\text{-C}(22)$).

$^{13}\text{C NMR}$ (101 MHz, CDCl_3) δ (ppm) = 190.9 (C(7)), 137.8 (C(21)), 137.7 (C(19)), 135.8 (C(10)), 134.1 (C(14)), 133.9 (C(18)), 130.1(C(6)), 129.9 (C(5, 11)), 129.8 (C(9)), 128.6 (C(20)), 128.1 (C(12)), 127.9 (C(8)), 127.0 (C(2)), 126.9 (C(4)), 126.7 (C(3)), 125.4 (C(7)), 125.4 (C(1)), 124.9 (C(13)), 36.4 (C(16)), 21.4 (C(23)), 20.2 (C(22)).f

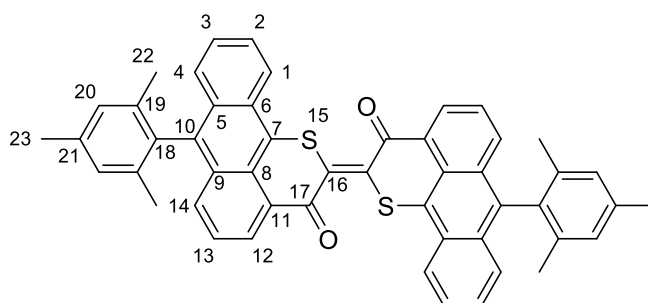
R_f = 0.47 (SiO_2 , *i*-hex : EtOAc 95:5).

HRMS (APPI), $[\text{MH}]^+$: m/z calc.: 369.1308 for $[\text{C}_{25}\text{H}_{21}\text{OS}]^+$, found: 369.1318.

m. p.: 80 – 82 °C.

IR: $\tilde{\nu}$ (cm^{-1}) = 2915.3 (w), 1681.5 (s), 1609.0 (w), 1519.5 (w), 1401.7 (w), 1372.5 (w), 1347.0 (w), 1277.6 (m), 1089.1 (w), 1060.4 (w), 1023.6 (w), 983.0 (w), 938.3 (w), 906.0 (w), 850.6 (m), 756.2 (s), 760.4 (s), 668.3 (m), 632.3 (m), 609.8 (w), 591.8 (w).

Peri-anthracenethioindigo (PAT 1)



6 (287 mg, 0.78 mmol, 2.0 equiv.) was dissolved in EtOH (30 mL) and aqueous NaOH (10%, 30 mL) and stirred at 70 °C for 3 h under air. After cooling to 23 °C the suspension was filtered and the solid was washed with water and hot MeOH. The product **1** was isolated as a green solid (189 mg, 0.51 mmol, 66%) in the *E* configuration.

E isomer:

¹H NMR (400 MHz, CDCl₃) δ (ppm) = 8.91 (d, *J* = 8.8 Hz, 1H, H-C(1)), 8.80 (dd, *J* = 7.1, 1.2 Hz, 1H, H-C(12)), 7.77 (dd, *J* = 8.6, 1.2 Hz, 1H, H-C(14)), 7.61 (d, *J* = 8.7 Hz, 1H, H-C(4)), 7.23 (ddd, *J* = 7.7, 6.5, 1.2 Hz, 1H, H-C(2)), 7.08 (ddd, *J* = 7.8, 6.5, 1.2 Hz, 1H, H-C(3)), 7.05 (dd, *J* = 8.6, 7.1 Hz, 1H, H-C(13)), 6.97 (s, 2H, H-C(20)), 2.32 (s, 3H, H₃-C(23)), 1.70 (s, 6H, H₃-C(22)).

¹³C NMR (101 MHz, CDCl₃) δ (ppm) = 181.7 (C(17)), 137.8 (C(19), C(21)), 135.3 (C(10)), 134.4 (C(18)), 133.3 (C(14)), 132.0 (C(16)), 130.7 (C(12)), 130.2 (C(5), C(9)), 129.8 (C(11)), 129.0 (C(20)), 128.8 (C(6)), 127.2 (C(2)), 127.0 (C(3), C(4)), 126.4 (C(13)), 125.4 (C(8)), 125.3 (C(7)), 124.2 (C(1)), 21.3 (C(22)), 20.1 (C(23)).

R_f = 0.50 (SiO₂, *i*-hex : EtOAc 95:5).

HRMS (MALDI), [M]: *m/z* calc.: 732.2157 for [C₅₀H₃₆O₂S₂], found: 732.2151.

Decomposition: 367 – 369 °C.

IR: $\tilde{\nu}$ (cm⁻¹) = 2911.6 (*w*), 1522.1 (*w*), 1396.6 (*w*), 1268.5 (*s*), 1162.2 (*w*), 1125.7 (*m*), 112.4 (*m*), 1067.3 (*m*), 937.8 (*m*), 894.2 (*m*), 852.9 (*m*), 823.5 (*w*), 753.3 (*s*), 663.3 (*m*), 650.9 (*m*), 632.9 (*m*), 553.0 (*m*).

Z isomer:

¹H NMR (400 MHz, CDCl₃) δ (ppm) = 8.66 (dd, *J* = 6.9, 1.3 Hz, 1H), 8.52 (dt, *J* = 8.8, 0.9 Hz, 1H), 7.74 (dd, *J* = 8.6, 1.3 Hz, 1H), 7.63 (dt, *J* = 8.8, 1.0 Hz, 1H), 7.30 – 7.23 (*m*, 3H), 7.10 – 7.02 (*m*, 3H), 7.01 – 6.94 (*m*, 3H), 2.33 (*s*, 4H), 1.70 (*s*, 6H).

Thermal isomerization

The *E* isomer of PAT is the thermodynamically most stable form. At elevated temperatures the metastable *Z* isomer is interconverting into the *E* isomer. The thermal stability of the metastable isomer *Z* was determined by heating a sample of the enriched *Z* isomer in benzene-*d*₆ or THF solution at 40 °C. After distinct time intervals the thermal *Z/E* isomerization was monitored by ¹H NMR spectroscopy or UV/Vis spectroscopy to determine the isomeric ratio. The first-order rate constant for the thermal *E* to *Z* isomerization was determined from the decay kinetics of the *Z* isomer during heating.

By using the *Eyring* equation (eq. 1) the Gibbs energy of activation ΔG^\ddagger can be calculated from the rate constant *k* of the reaction:

$$k = \frac{k_B T}{h} e^{\frac{-\Delta G^\ddagger}{RT}} \quad \text{eq. 1}$$

With k_B = Boltzmann constant ($1.381 \cdot 10^{-23} \text{ J} \cdot \text{K}^{-1}$)

T = temperature in K

h = Planck constant ($6.626 \cdot 10^{-34} \text{ J} \cdot \text{s}$)

k = rate constant of the reaction

Eq. 1 can be rearranged and the numerical value of the rate constant can then be inserted into eq. 2:

$$\Delta G^\ddagger (\text{in } \text{J mol}^{-1}) = -\ln\left(\frac{k h}{k_B T}\right) R T \quad \text{eq. 2}$$

The half-life time of the metastable *Z* isomer is calculated by dividing $\ln(2)$ by the rate constant *k*, see eq. 3.

$$t_{1/2} = \frac{\ln(2)}{k} \quad \text{eq. 3}$$

To calculate the relative energy differences ΔG between the two isomeric states the equilibrium constant *K* must be inserted into eq 4, with $K = ([Z]/[E])$ after thermal decay.

$$-\Delta G = \ln(K) R T \quad \text{eq. 4}$$

Since no residual Z isomer is observed after thermal isomerization a lower limit for the relative energy differences ΔG between the two isomeric states is obtained when inserting $K = ([Z]/[E]) = (5/95)$, by which it is assumed that remaining 5% of the metastable Z isomer is not observed in the NMR experiment. This conservative estimation gives a value of $\Delta G = \geq 2.0$ kcal/mol.

In case the thermal isomerizations do not proceed to 100% in one direction but are instead dynamic equilibria the observed decays are composites of both isomerization processes (*E* to *Z* and *vice versa*) and have to be analyzed as previously reported.^[2]

Table S1 Gibbs energy of activation ΔG^\ddagger of the thermal Z to E isomerization of **1**, corresponding half-life $t_{1/2}$ of the Z isomer and lower limit for the relative energy difference between the two isomeric states ΔG . Thermal Z to E decays were measured in benzene-*d*₆ or THF at 40 °C. Isomeric ratio *E* : Z after thermal decay is determined by ¹H NMR spectroscopy (benzene-*d*₆) or UV/Vis spectroscopy (THF).
^a Linearly extrapolated to 20 °C.

	ΔG^\ddagger (therm.) Z/E [kcal mol ⁻¹]	T [°C]	$t_{1/2}$ [h]	<i>E</i> _{end} [%]	ΔG [kcal mol ⁻¹]
benzene- <i>d</i> ₆	24.3	40 (20) ^a	2.7 (2 d) ^a	≥95	≥2.0
THF	25.8	40 (20) ^a	4.3 h (23 d) ^a	≥22	≥0.9

Figure S1 - Figure S6 show the thermal isomerization of metastable Z isomer to stable isomer *E* isomer in the dark followed by ¹H NMR spectroscopy and corresponding kinetic plots of the Z/E-conversion of isomers during heating over time in benzene-*d*₆ at 40 °C.

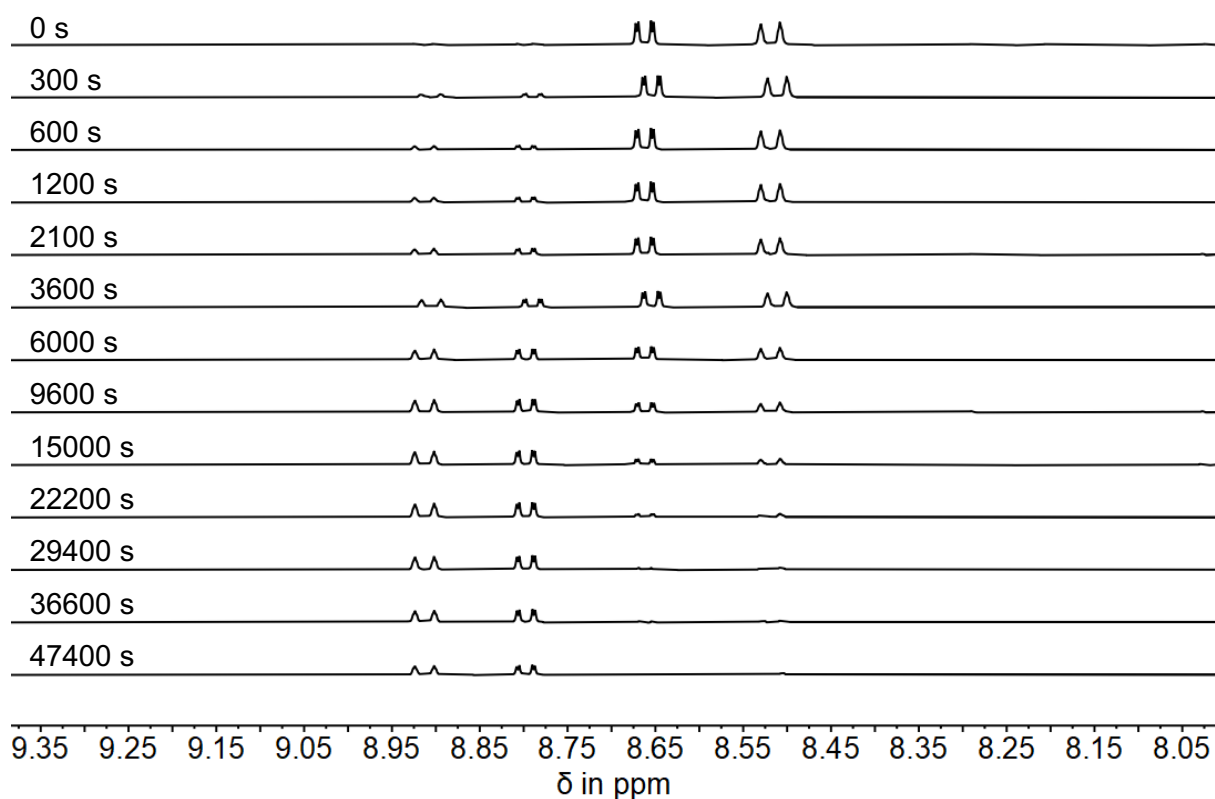


Figure S1 Thermal isomerization of PAT Z-1 followed by ^1H NMR spectroscopy in regular time intervals in benzene- d_6 at 40 °C. Partial ^1H NMR spectra (400 MHz, benzene- d_6 , 25 °C) recorded during the conversion of metastable isomer Z to stable isomer E.

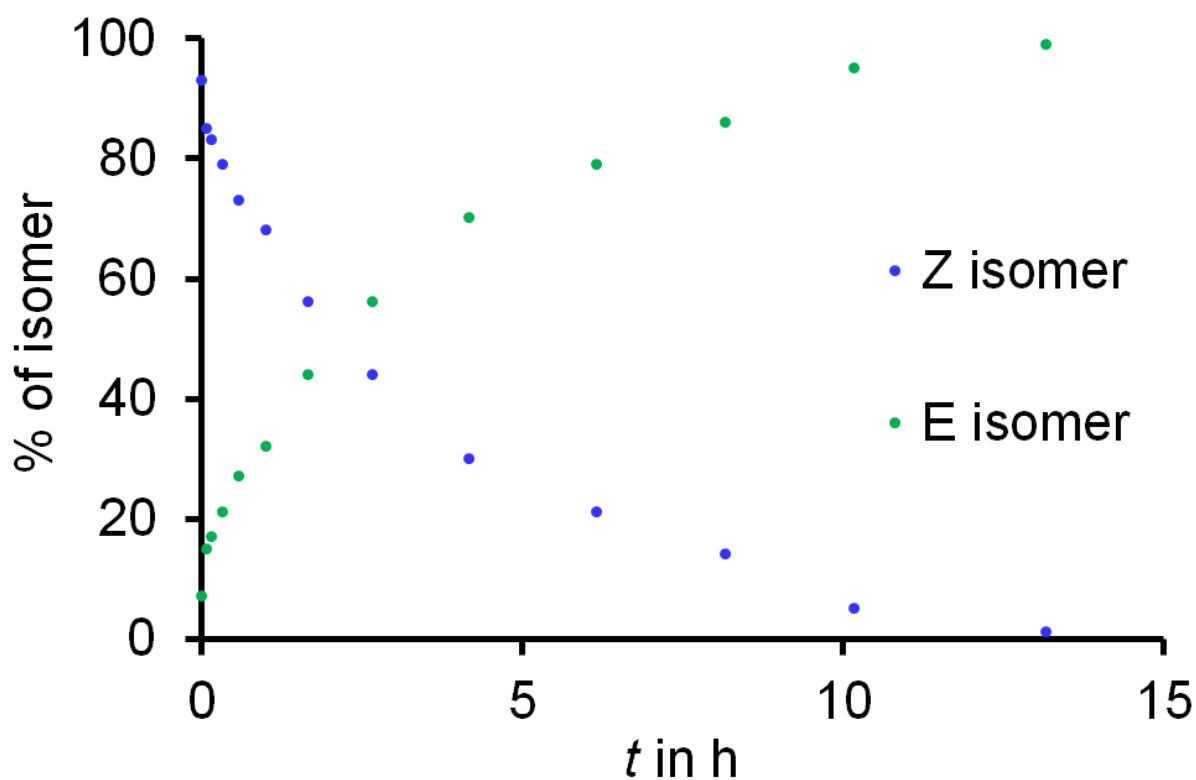


Figure S2 Changing isomer ratio during thermally induced conversion of metastable isomer Z-1 to stable isomer E-1 in benzene- d_6 at 40 °C.

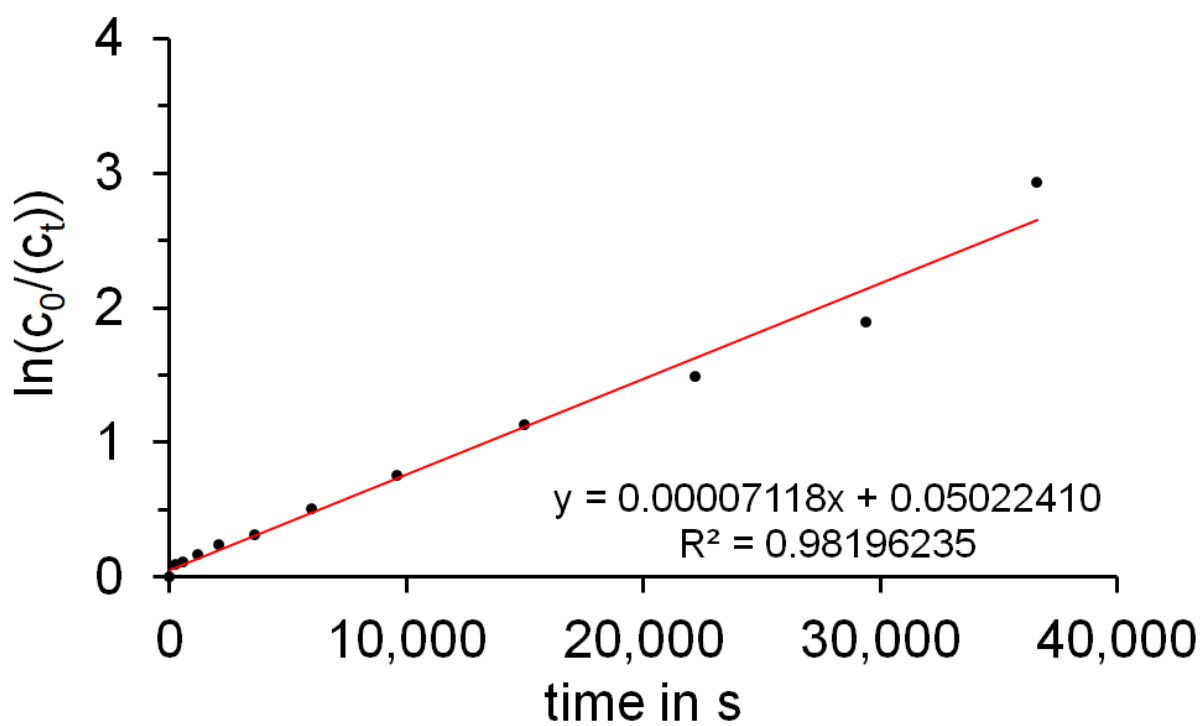


Figure S3
to 40 °C.

Linearized kinetic plot of decreasing Z isomer in benzene- d_6 during heating in the dark

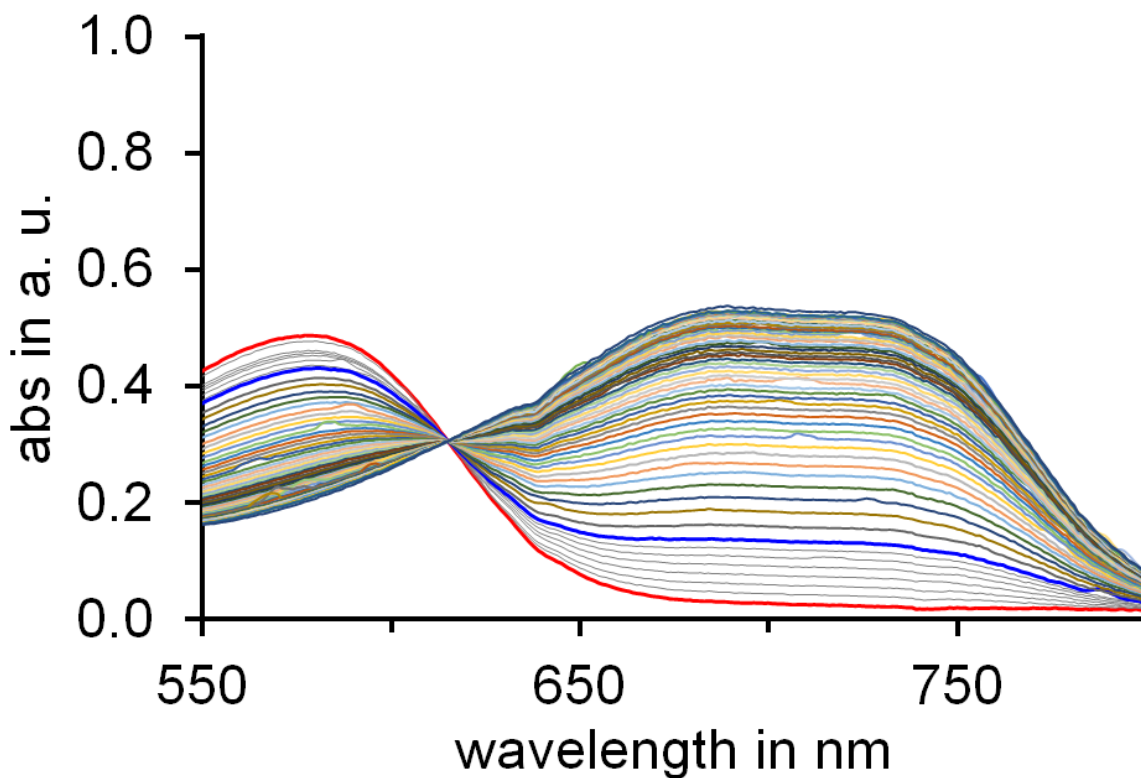


Figure S4 Thermal isomerization of PAT Z-1 followed by UV/Vis spectroscopy in regular time intervals in THF at 40 °C. UV/Vis spectra recorded during the conversion of metastable isomer Z to stable isomer E.

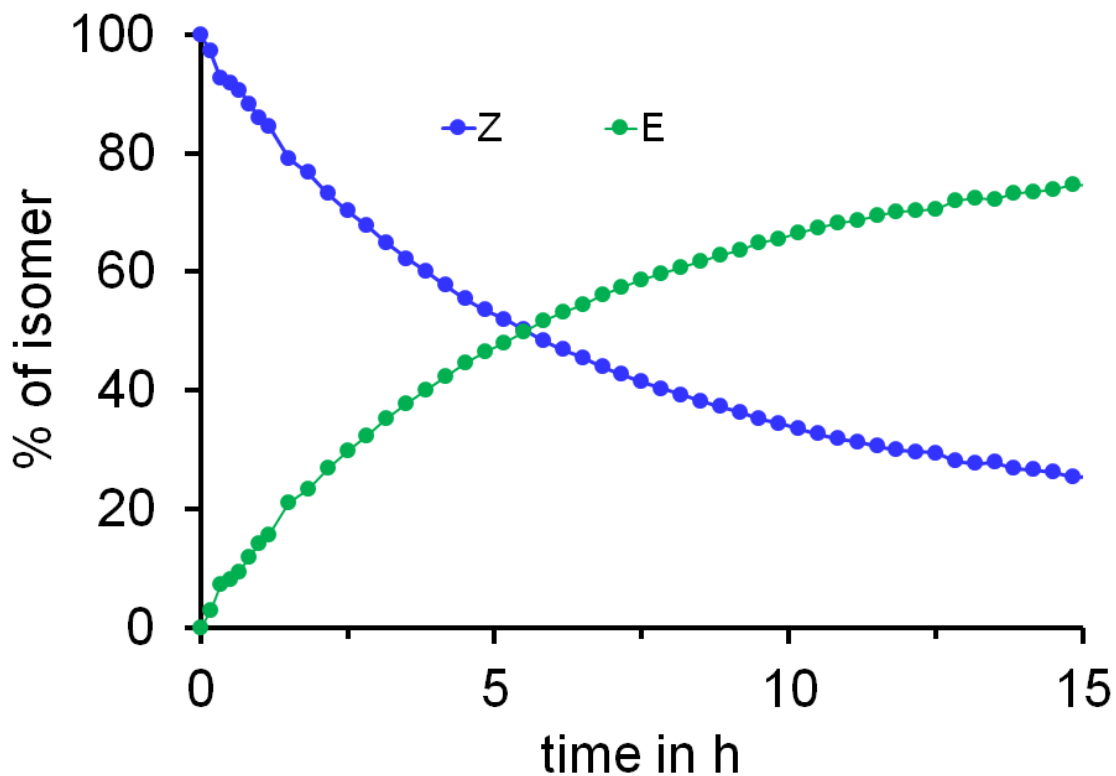


Figure S5 Changing isomer ratio during thermally induced conversion of metastable isomer Z-1 to stable isomer E-1 in THF at 40 °C.

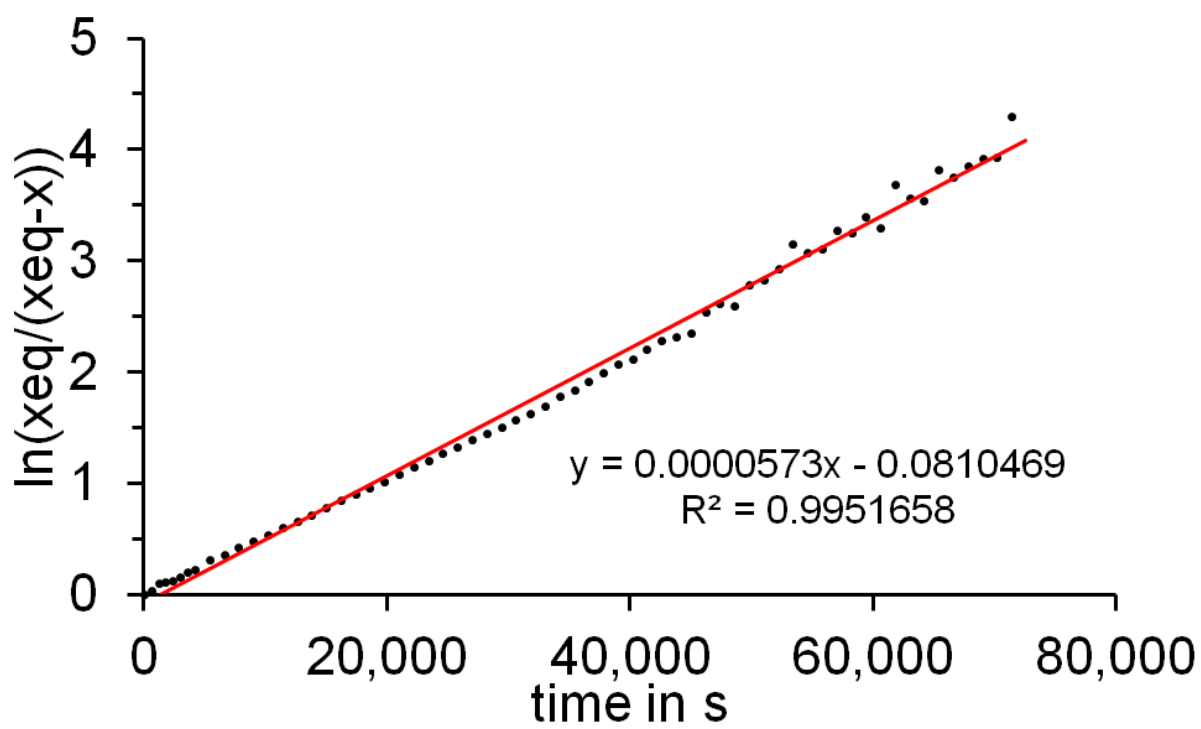


Figure S6 Linearized kinetic plot of decreasing Z isomer in THF during heating in the dark to 40 °C.

Photophysical and photochemical properties

PSS determination using ^1H NMR spectroscopy

The photostationary state (pss) was determined in benzene- d_6 at 23 °C by ^1H NMR spectroscopy. Therefore, **1** was dissolved in deuterated benzene and irradiated with light of different wavelengths for distinct time intervals until no further change was observed. After each irradiation step a ^1H NMR spectra was measured to determine the isomeric ratio.

Table S2 gives an overview over the isomeric ratios of **1** obtained after irradiation with light of different wavelengths to the respective pss in benzene- d_6 .

Table S2 Isomer yields of **1** obtained after irradiation with light of different wavelengths until the respective pss was reached. Isomeric ratios were determined in benzene- d_6 solutions at 23 °C using ^1H NMR spectroscopy.

λ $E \rightarrow Z$	$E : Z$	λ $Z \rightarrow E$	$E : Z$
780 nm	0 : 100	617 nm	72 : 28
730 nm	1 : 99	590 nm	87 : 13
720 nm	3 : 97	550 nm	83 : 17

Figure S7 shows ^1H NMR spectra of **1** before and after irradiation at 23 °C in benzene- d_6 . Starting with 100% of the stable E isomer, the metastable Z isomer can be enriched by irradiating with light >680 nm. Using a different wavelength the reverse Z/E photoisomerisation occurs.

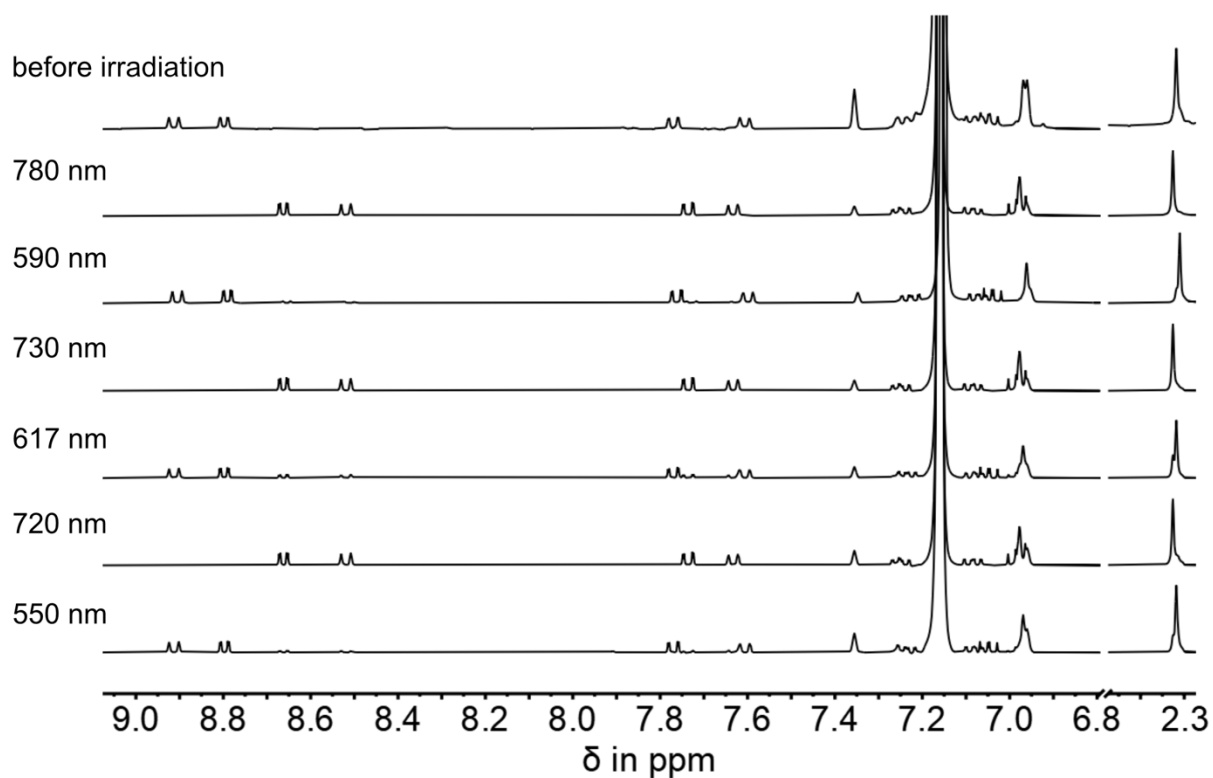


Figure S7 ¹H NMR spectra (400 MHz, benzene-*d*₆, 23 °C) of **1** before and after irradiation with different wavelengths. The sample was irradiated with one wavelength until no further change of the isomeric ratio was observed and therefore the pss was reached. Subsequently the sample was irradiated with a complementary wavelength to instill the reverse photoisomerization.

PSS determination using UV/Vis spectroscopy

The photostationary state (pss) was determined in benzene and THF at 23 °C by UV/Vis spectroscopy. Therefore, **1** was dissolved in benzene or THF and irradiated with light of different wavelengths for distinct time intervals until no further change was observed. After each irradiation step a UV/Vis spectra was measured to determine the isomeric ratio using the molar absorption coefficient.

Table S3 gives an overview over the isomeric ratios of **1** obtained after irradiation with light of different wavelengths to the respective pss in benzene-*d*₆.

Table S3 Isomer yields of **1** obtained after irradiation with light of different wavelengths until the respective pss was reached. Isomeric ratios were determined in benzene and THF solutions at 23 °C using UV/Vis spectroscopy.

	λ <i>E</i> → <i>Z</i>	<i>E</i> : <i>Z</i>	λ <i>Z</i> → <i>E</i>	<i>E</i> : <i>Z</i>
benzene	780 nm	0 : 100	625 nm	69 : 31
	730 nm	1 : 99	590 nm	91 : 9
	720 nm	1 : 99	554 nm	86 : 13
THF	780 nm	0 : 100	617 nm	65 : 35
	730 nm	0 : 100	590 nm	83 : 17
	720 nm	0 : 100	550 nm	80 : 20

Photoisomerization followed by UV/Vis spectroscopy

Figure S8 and Figure S9 show UV/Vis spectra measured before and after irradiation of **1** in benzene or THF at 23 °C. A solution of **1** was prepared in UV/Vis concentration in a 10 mm pathlength cuvette. Starting from the pure *E* isomer, the metastable *Z* isomer is enriched by irradiating. Using a different wavelength the reverse *Z* to *E* photoisomerisation occurs.

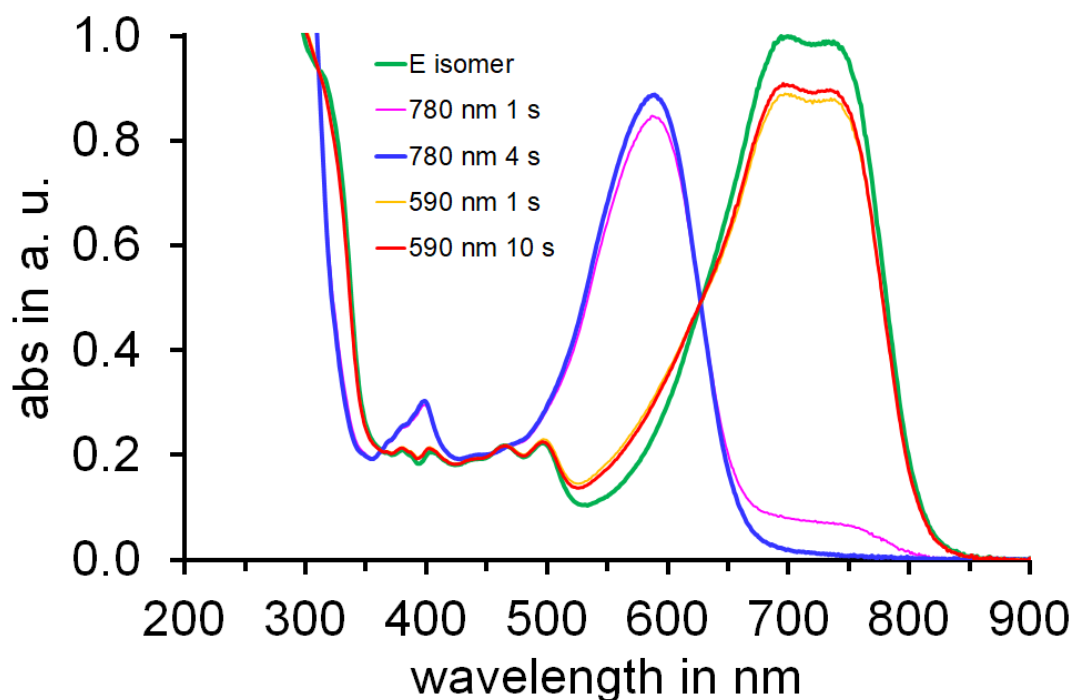


Figure S8 Absorption spectra of PAT **1** recorded before and after irradiation in benzene solution at 23 °C. Starting from the stable *E* isomer the metastable *Z* isomer can be enriched using 780 nm red light. After irradiation with 590 nm orange light the reverse *Z/E* isomerization occurs and the *E* isomer is enriched.

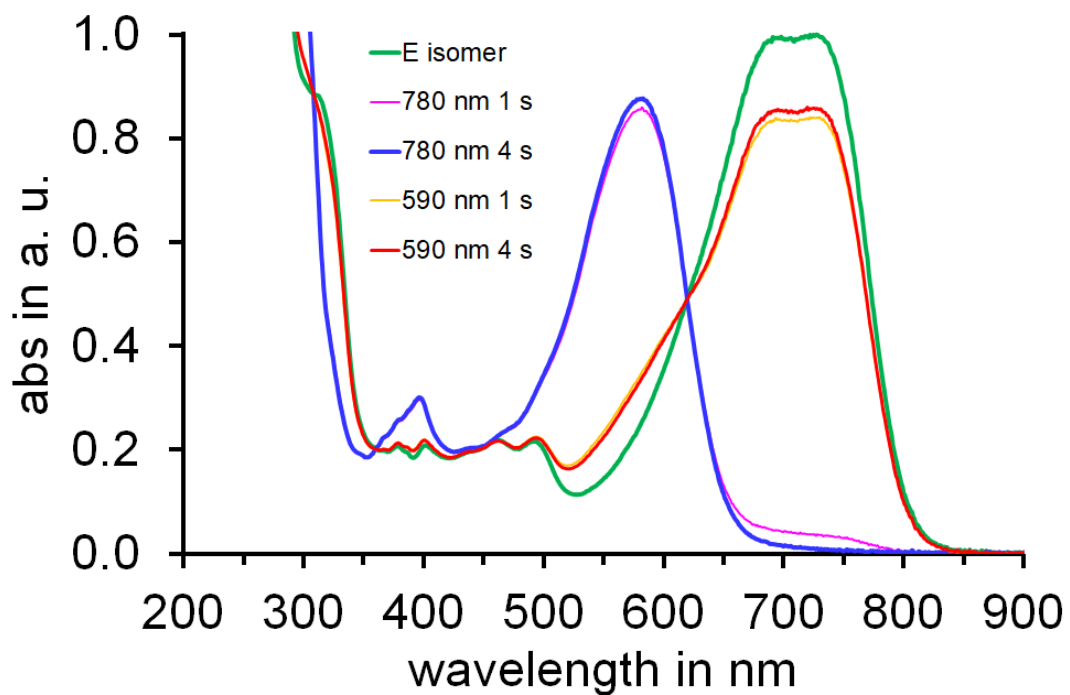


Figure S9 Absorption spectra of PAT 1 recorded before and after irradiation in THF solution at 23 °C. Starting from the stable *E* isomer the metastable *Z* isomer can be enriched using 780 nm red light. After irradiation with 590 nm orange light the reverse *Z/E* isomerization occurs and the *E* isomer is enriched.

Molar absorption coefficients

The molar absorption coefficients ϵ of PAT isomers *E*-**1** and *Z*-**1** were obtained directly from isomerically pure material using the *Lambert-Beer* law. A solution with a known concentration of the pure *E* isomer was prepared with benzene and THF and the absorption spectra was measured. Next the sample was irradiated with a suitable red light LED to enrich the *Z* isomer quantitatively and the absorption spectra was measured again. Table S4 summarizes the maximum wavelengths of the lowest energy absorption band and the corresponding molar absorption coefficients in different solvents at 23°C, as well as the difference of the maximum wavelength $\Delta\lambda_{\max}$ of the most redshifted absorption band between *Z* and *E* isomer.

Table S4 Quantitative comparison of the maximum wavelength λ_{\max} and molar absorption coefficients ϵ of the most redshifted absorption bands of *E*-**1** and *Z*-**1** in benzene and THF. Absolute difference $\Delta\lambda_{\max}$ between maximum wavelength of *E* isomer $\lambda_{\max(E)}$ and *Z* isomer $\lambda_{\max(Z)}$ of most redshifted absorption are also shown. Data were measured in benzene, tetrahydrofuran, CH₂Cl₂ and pyridine solutions at 23°C.

	<i>E</i> isomer		<i>Z</i> isomer		$\Delta\lambda_{\max}$ [nm]
	λ_{\max} [nm]	ϵ [L mol ⁻¹ cm ⁻¹]	λ_{\max} [nm]	ϵ [L mol ⁻¹ cm ⁻¹]	
benzene	701	24,800	591	22,000	110
THF	724	23,100	581	20,000	143

The molar absorption coefficient of **1** in benzene is shown in Figure S10.

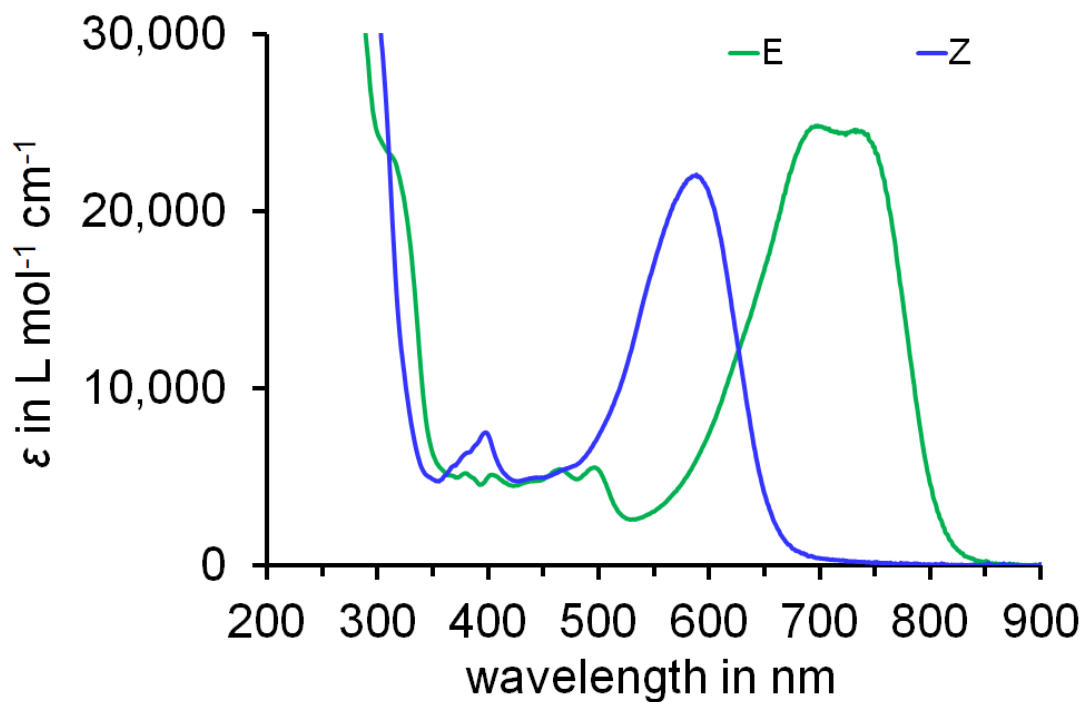


Figure S10 Molar absorption coefficients ϵ of **1** in benzene at 23 °C. The *E* isomer is displayed in green, the *Z* isomer is displayed in blue.

The molar absorption coefficient of **1** in THF is shown in Figure S11.

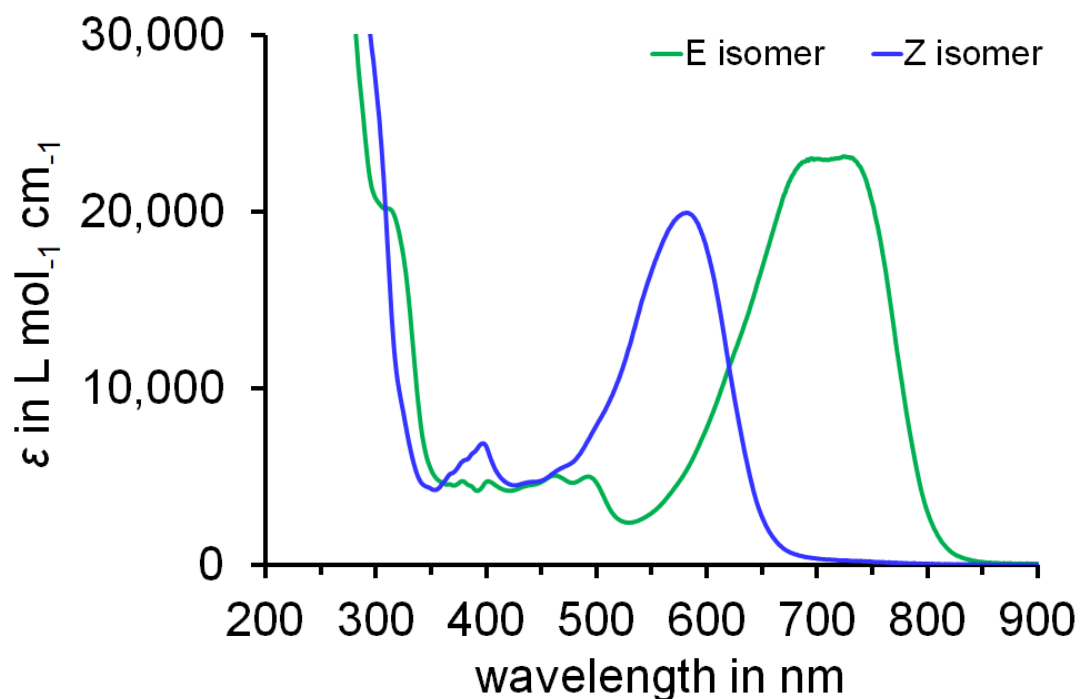


Figure S11 Molar absorption coefficient ϵ of **1** in THF at 23 °C. The *E* isomer is displayed in green, the *Z* isomer is displayed in blue.

Quantum Yield Determination

The photochemical quantum yield of the *E/Z* photoisomerization $\Phi_{E\rightarrow Z}$ and the *Z/E* photoisomerization $\Phi_{Z\rightarrow E}$, respectively were determined by using an updated instrumental setup developed by the group of *E. Riedle*.^[3] The photochemical quantum yield Φ of a particular wavelength is calculated from the ratio between the number of isomerized molecules and the number of absorbed photons, according to equation 2:

$$\Phi = \frac{N(\text{isomerized molecules})}{N(\text{absorbed photons})} \quad \text{eq. 2}$$

A solution of PAT **1** in benzene or THF (2.00 mL) was prepared in a cuvette. The sample was irradiated at the isosbestic point (IP) with a suitable wavelength for distinct time intervals after which the power and the degree of isomerization by UV/Vis spectroscopy were measured. The determined values of the photochemical quantum yields $\Phi_{E\rightarrow Z}$ and $\Phi_{Z\rightarrow E}$ are shown in Table S5.

Table S5 Comparison of photochemical quantum yield of *E* to *Z* isomerization $\Phi_{E\rightarrow Z}$ and *Z* to *E* isomerization $\Phi_{Z\rightarrow E}$ of PAT **1** in benzene and THF solution.

	$\Phi_{E\rightarrow Z}$	$\Phi_{Z\rightarrow E}$	λ_{LED}
benzene	9%	26%	619 nm
THF	12%	31%	619 nm

Starting from a *Z/E* mixture the photochemical quantum yields $\Phi_{Z\rightarrow E}$ and $\Phi_{E\rightarrow Z}$ of **1** were measured by irradiating the sample ($c = 3 \cdot 10^{-5} \text{ mol L}^{-1}$) with 619 nm (1.89 V, 0.10 A). UV/Vis spectra were taken immediately after irradiating for certain time intervals at 23 °C. The sample was irradiated for about 480 s in total. In Figure S12 and Figure S13 the *Z/E* isomerization as monitored by UV/Vis spectroscopy and the corresponding change of concentration of *Z* and *E* isomer over time is shown.

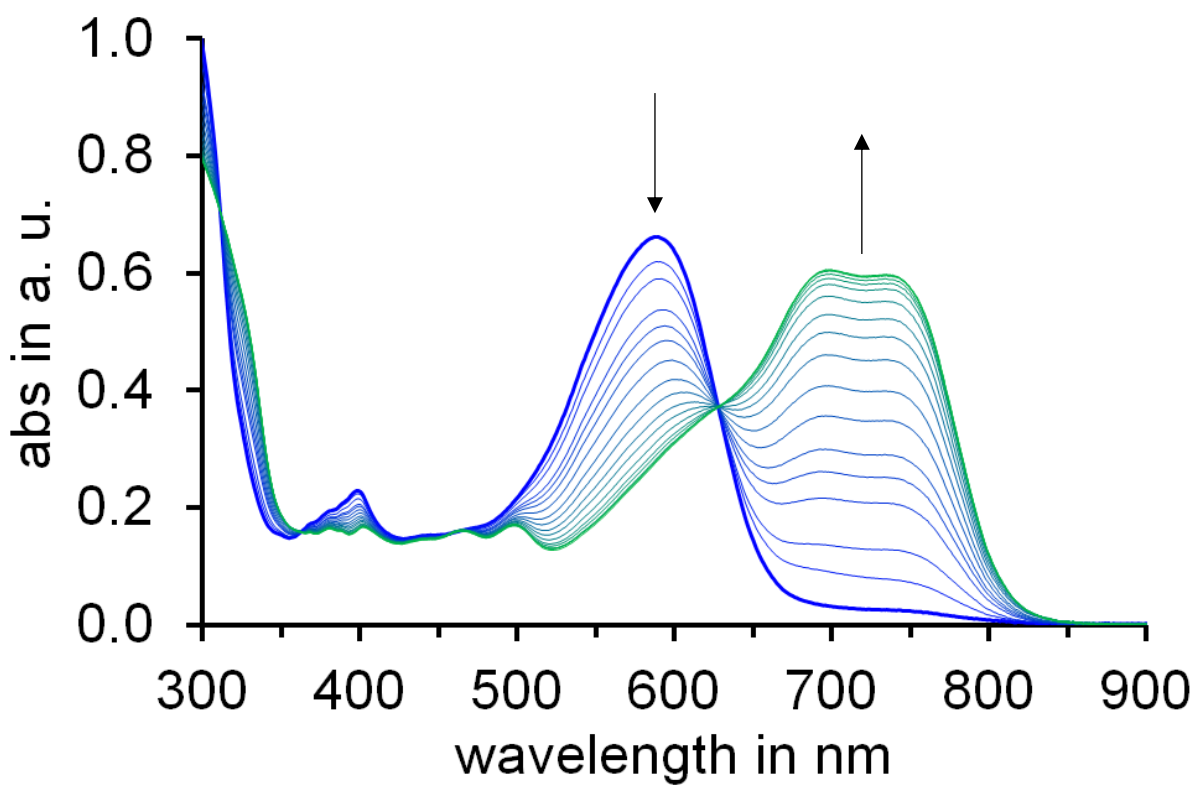


Figure S12 UV/Vis spectra recorded during the Z to E isomerization of 1 after irradiation with 619 nm for certain time intervals in benzene solution at 23 °C.

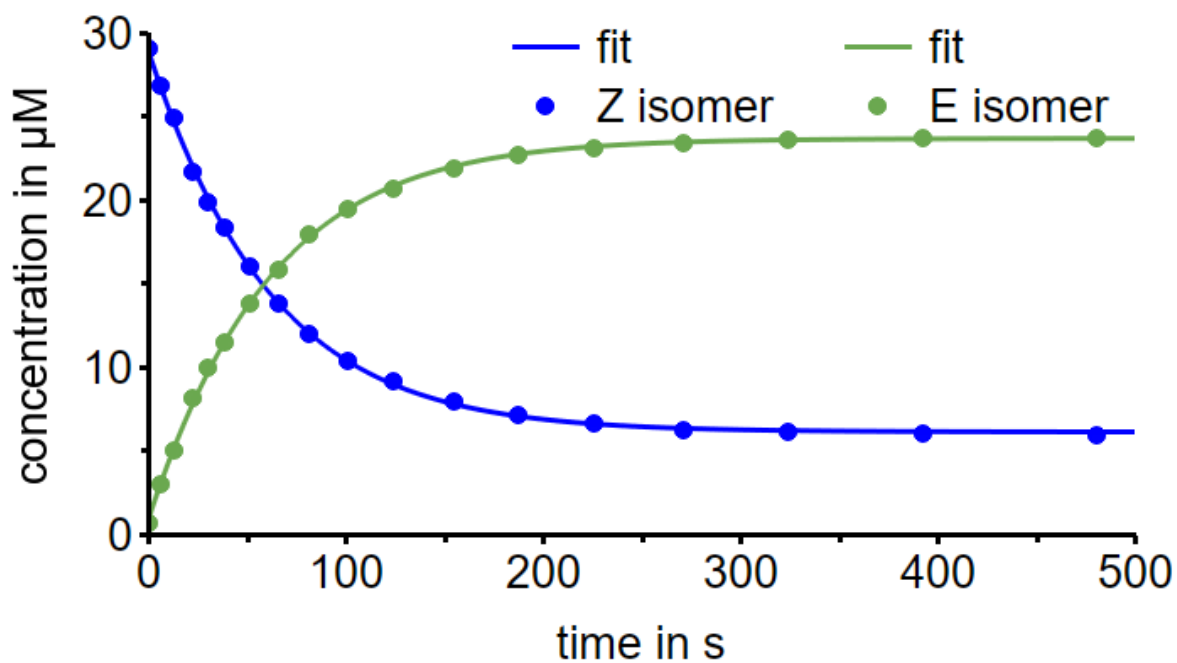


Figure S13 Change of concentration of the Z and E isomer of 1 after stepwise irradiating with 619 nm light for a total of 480 s in benzene solution.

Starting from a *Z/E* mixture the photochemical quantum yields $\Phi_{Z \rightarrow E}$ and $\Phi_{E \rightarrow Z}$ of **1** were measured in THF by irradiating the sample ($c = 3 \cdot 10^{-5} \text{ mol L}^{-1}$) with 619 nm (1.91 V, 0.10 A). UV Vis spectra were taken immediately after irradiating for certain time intervals at 23 °C. The sample was irradiated for about 550 s in total. In Figure S14 and Figure S15 the *Z/E* isomerization as monitored by UV/Vis spectroscopy and the corresponding change of concentration of *Z* and *E* isomer over time is shown.

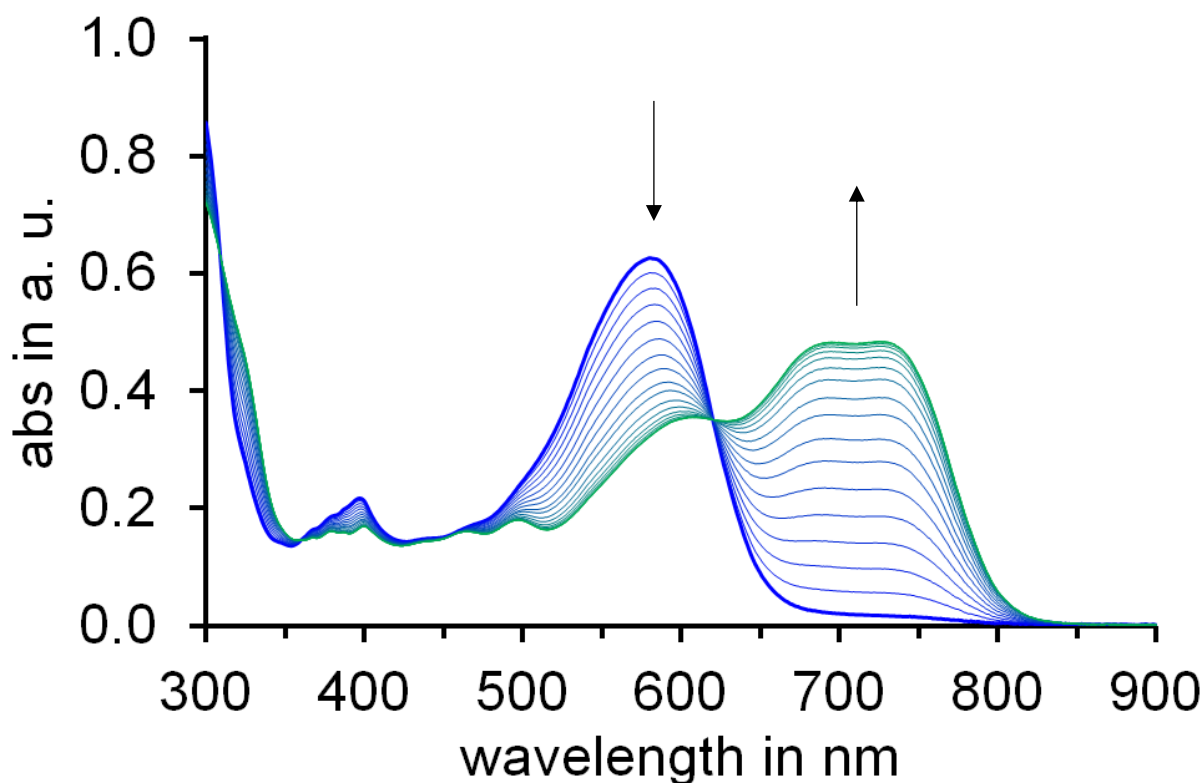


Figure S14 UV/Vis spectra recorded during the *Z* to *E* isomerization of **1** after irradiation with 619 nm for certain time intervals in THF solution at 23 °C.

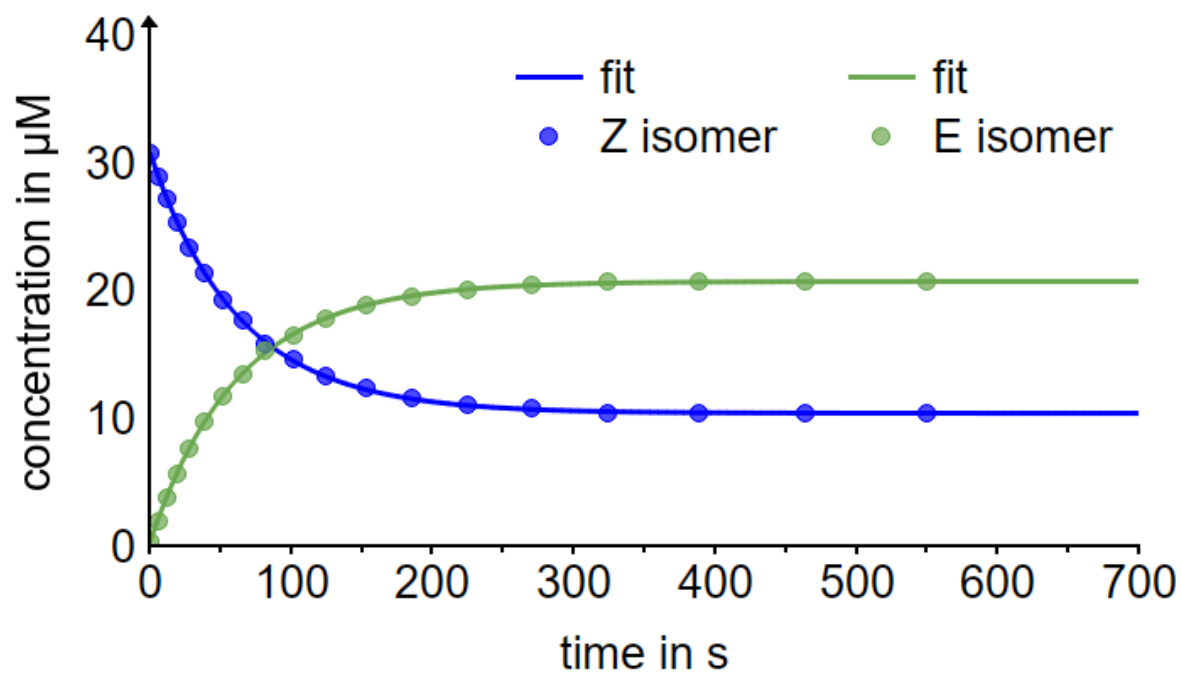


Figure S15 Change of concentration of the Z and E isomer of 1 after stepwise irradiating with 619 nm light for a total of 550 s in THF solution.

Photostability

To scrutinize the photostability of PAT **1** 15 reversible photoswitching cycles were performed followed by UV/Vis spectroscopy at 23 °C. Therefore, a sample of **1** was prepared in benzene in UV/Vis concentration. The sample was then alternately irradiated with 780 nm light (enrichment of Z isomer) and 590 nm light (enrichment of E isomer) until the pss was reached each time (10 s). After each irradiation an UV/Vis spectrum was measured. The absorbance of the two isomers at 700 nm and at the isosbestic point are compared for each cycle.

Figure S16 shows the 15 switching cycles of **1** in benzene solution.

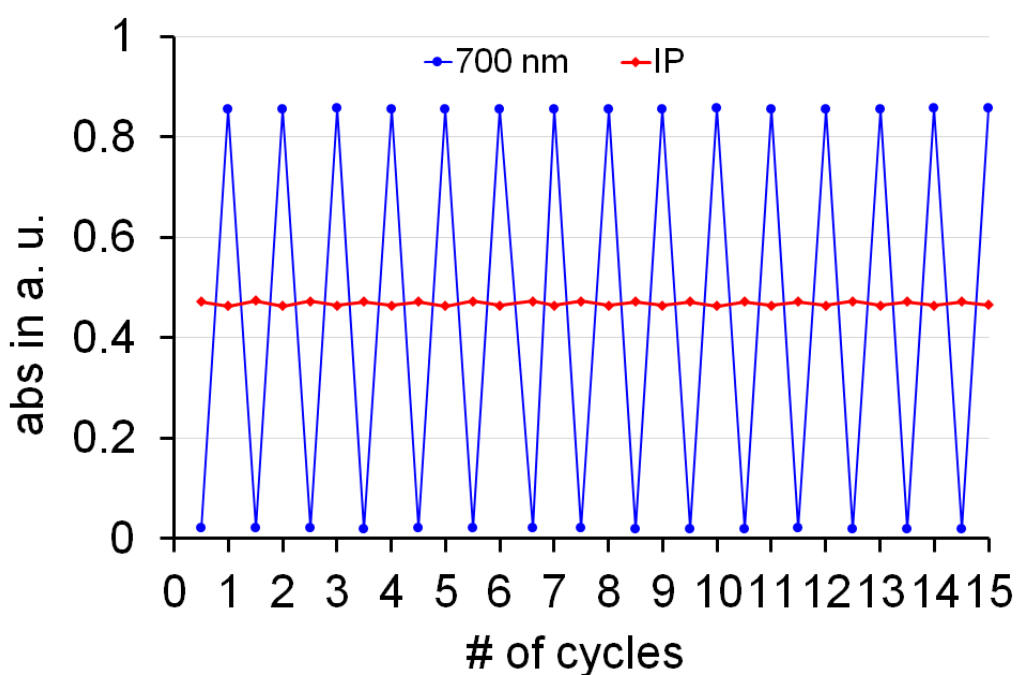


Figure S16 Change of absorption of PAT **1** at 700 nm and at the IP at 627 nm after alternating irradiation with 780 nm and 590 nm light in benzene solution at 23 °C. One photoswitching cycle consists of irradiation with 780 nm for 10 s to enrich the Z isomer and irradiation with 590 nm for 10 s to enrich the E isomer. After each irradiation step an UV/Vis spectrum was measured. The switching cycle was repeated 15 times.

Figure S17 shows the 15 switching cycles of **1** in THF.

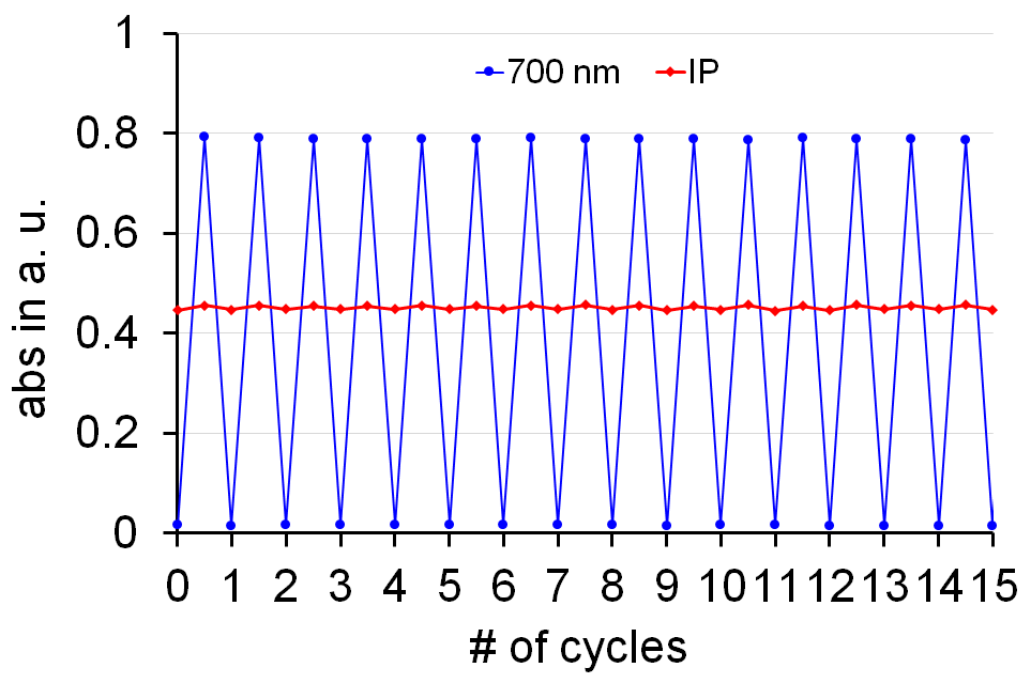


Figure S17 Change of absorption of PAT 1 at 700 nm and the IP at 620 nm after alternating irradiation with 780 nm and 590 nm in THF at 23 °C. One photoswitching cycle consists of irradiation with 780 nm for 10 s to enrich the *Z* isomer and irradiation with 590 nm for 10 s to enrich the *E* isomer. After each irradiation step a UV/Vis spectra was measured. The switching cycle was repeated 15 times.

Incorporation into Polymer and Photoswitching

PAT **1** was incorporated into a polystyrene polymer according to a procedure developed by *M. Sacherer*.^[2] Styrene (40 mL) was stirred at 140 °C for 40 min. *E*-**1** (4.0 mg) was dissolved in benzene (1.0 mL) and added to the polymer. The polymer was further stirred at 140 °C for 5 min. The mixture was poured into petri dishes and dried for 20 h at 23 °C.

Switching experiments were performed by irradiating a polymer with either 730 nm light to enrich the *Z* isomer or 590 nm light to enrich the *E* isomer, see Figure S18.

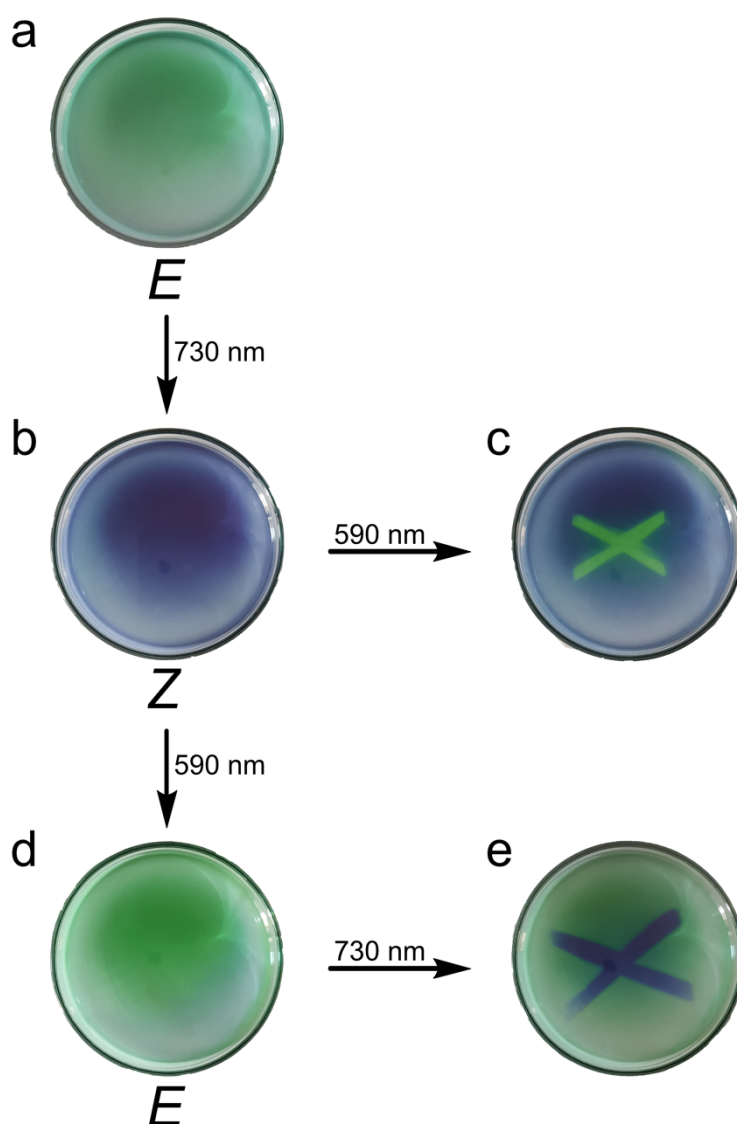
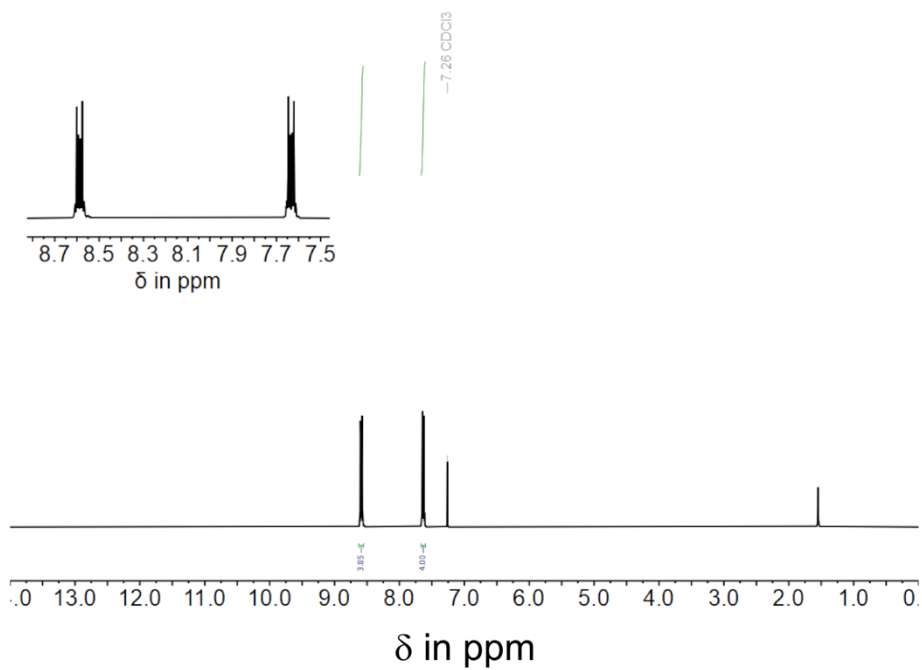


Figure S18 Embedded PAT **1** in polystyrene polymer. a Pure *E*-**1** isomer embedded in the polymer. b After irradiation with 730 nm to enrich the *Z*-**1** isomer is enriched (blue polymer). c Irradiation of the *Z*-**1** isomer with 590 nm in the shape of an "X". d After irradiation with 590 nm the *E*-**1** isomer was enriched (green polymer). e Irradiation of the *E*-**1** isomer with 730 nm in the shape of an "X".

NMR spectra

a



b

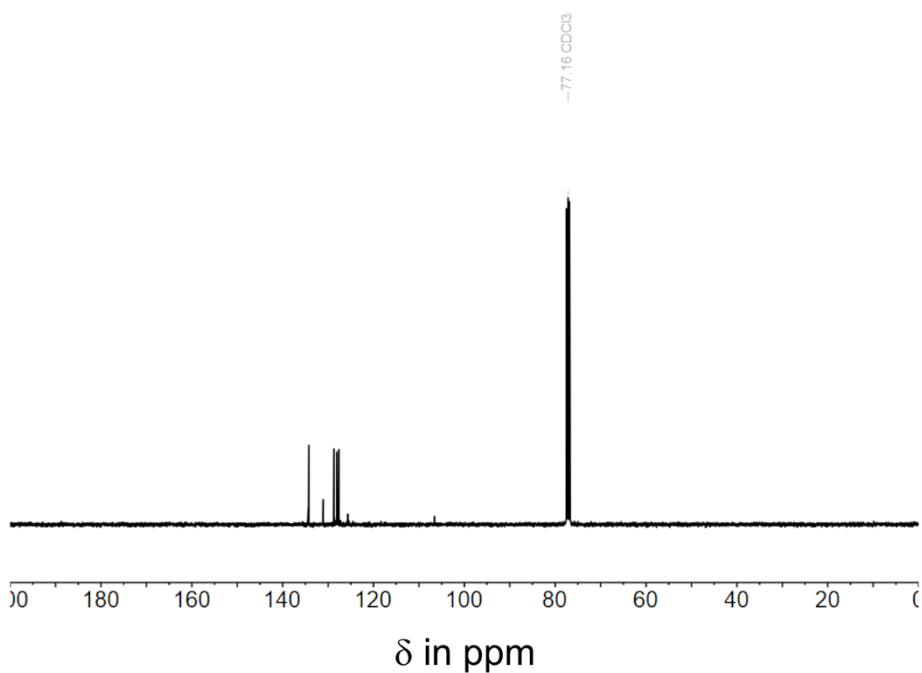


Figure S19 NMR spectra of **2** in CDCl_3 at 23 °C. a ^1H NMR spectrum (400 MHz). b ^{13}C NMR spectrum (101 MHz).

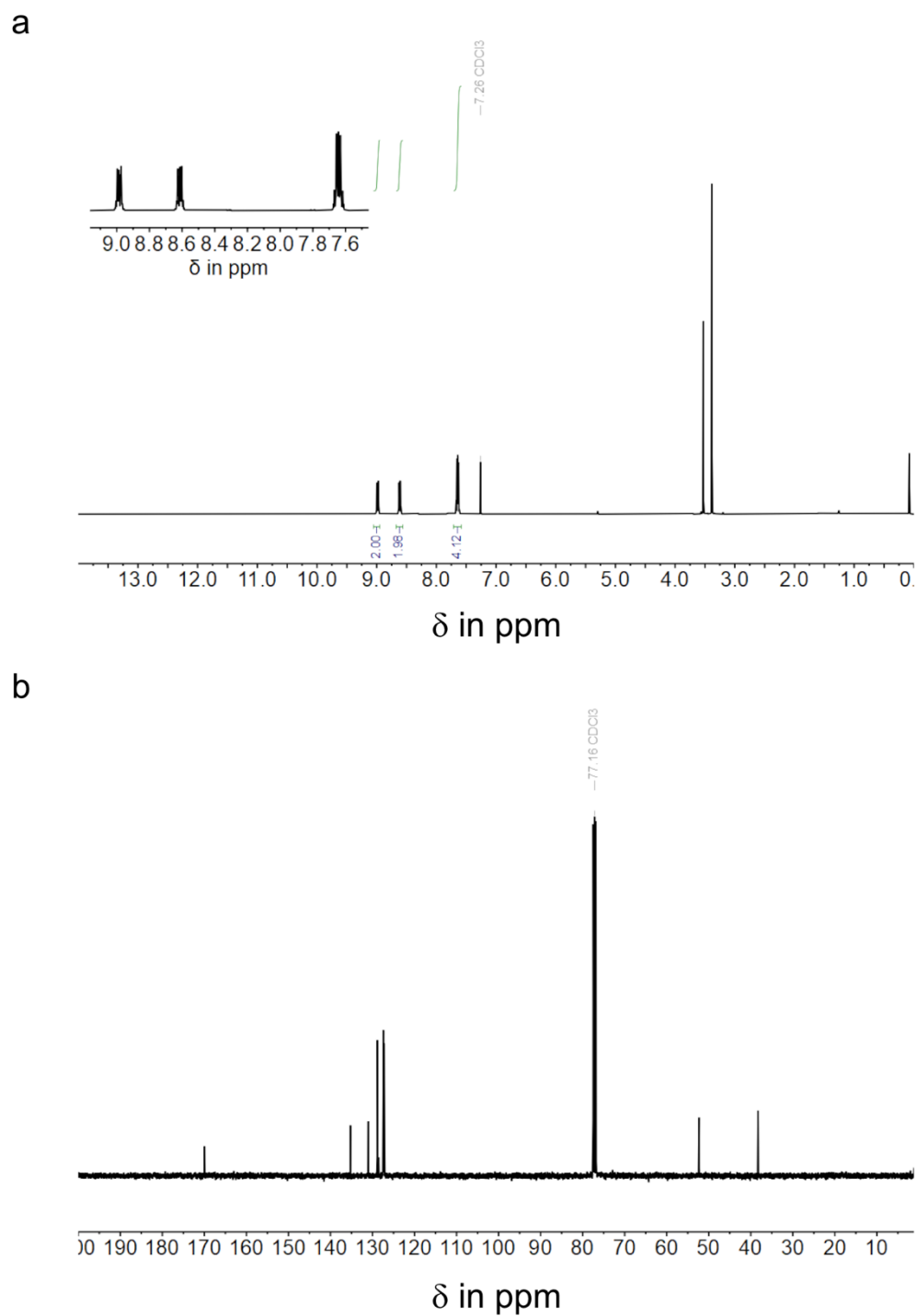


Figure S20 NMR spectra of **3** in CDCl_3 at 23 °C. a ^1H NMR spectrum (400 MHz). b ^{13}C NMR spectrum (101 MHz).

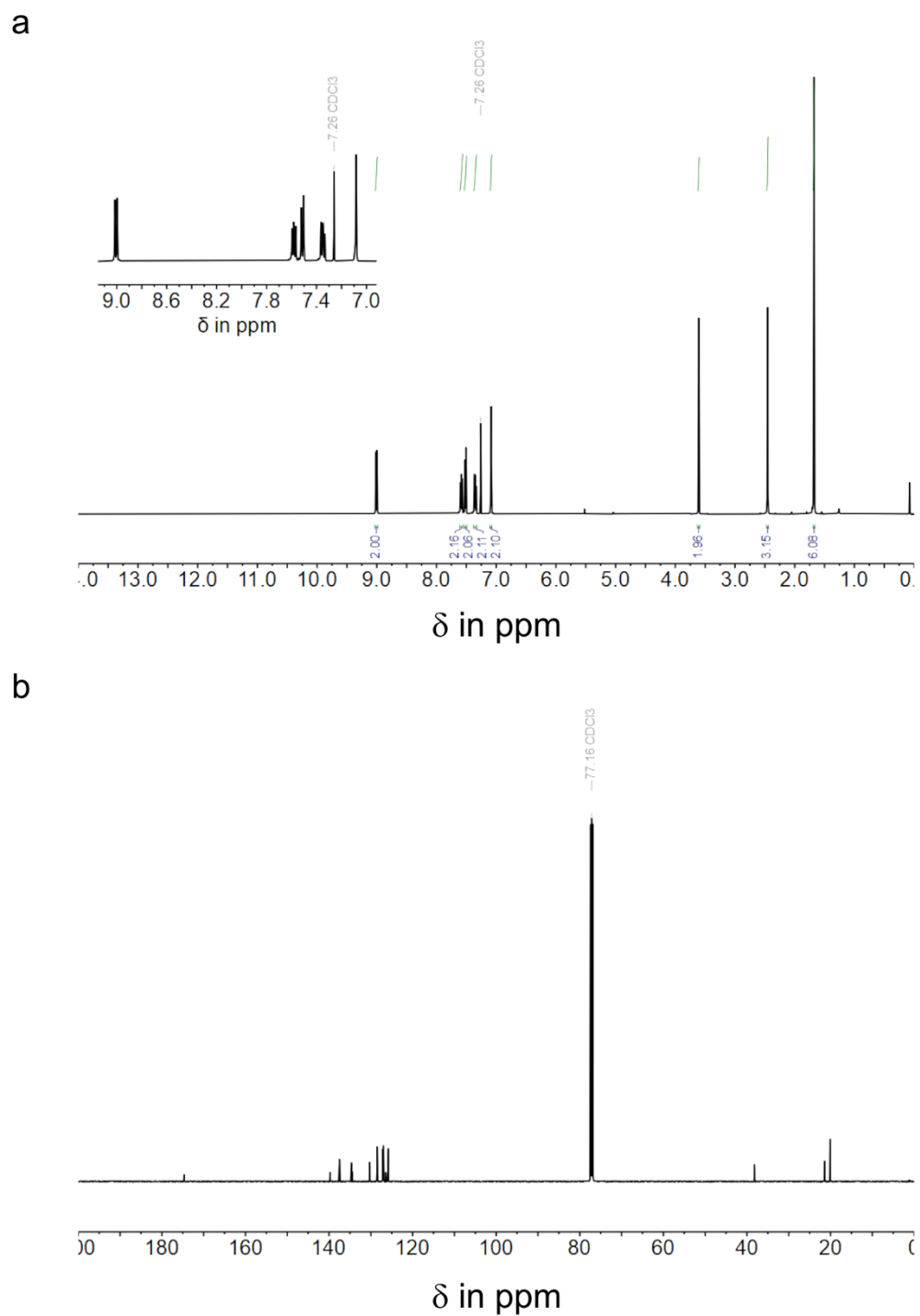


Figure S22 NMR spectra of **5** in CDCl_3 at 23 °C. a ^1H NMR spectrum (400 MHz). b ^{13}C NMR spectrum (101 MHz).

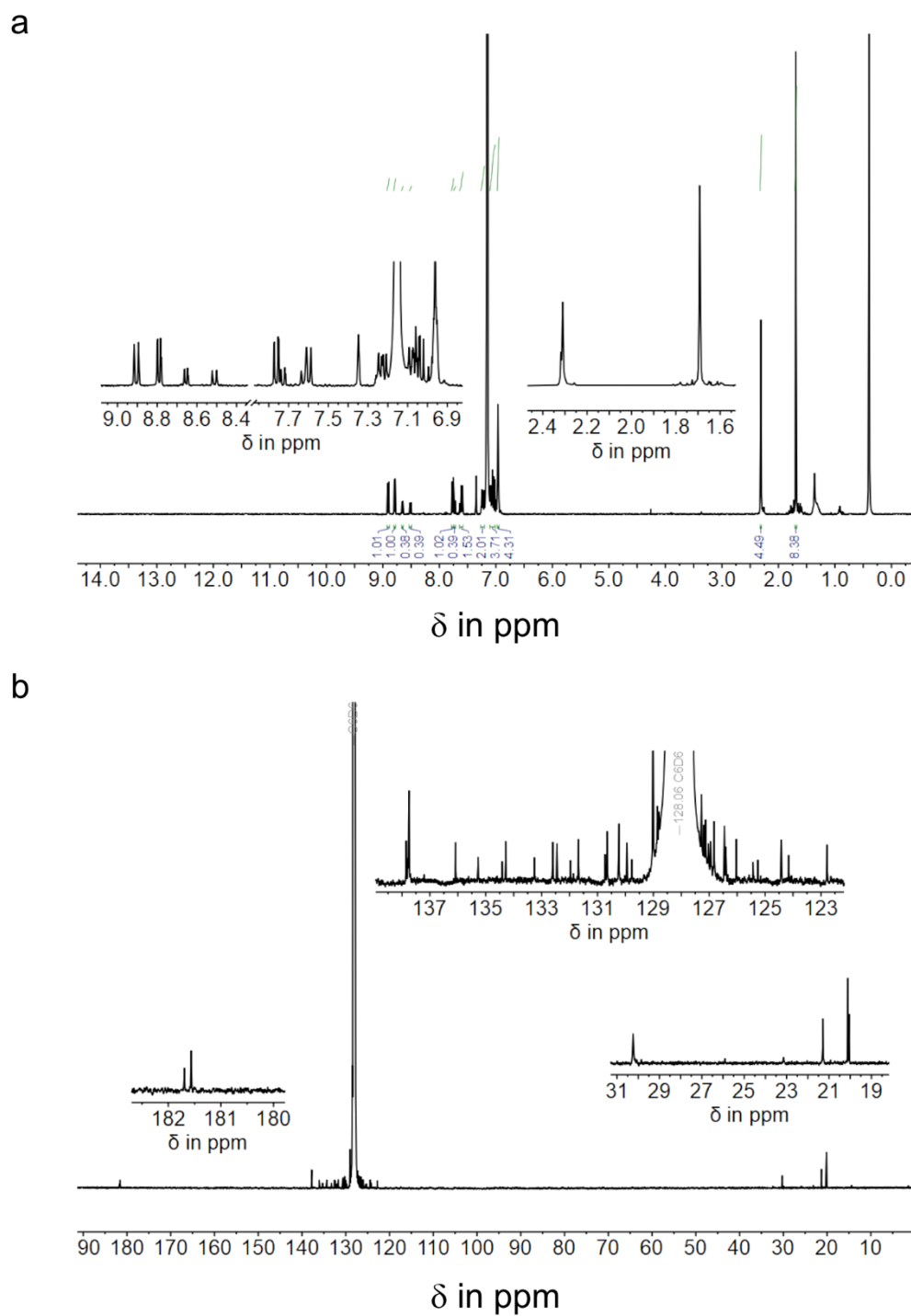


Figure S24 NMR spectra of **1** (mixture of *E* and *Z*) in C_6D_6 at 23 °C. a 1H NMR spectrum (400 MHz). b ^{13}C NMR spectrum (101 MHz).

References

- [1] T. Nishioka, K. Kuroda, M. Akita, M. Yoshizawa, *Angew. Chem. Int. Ed.* **2019**, *58*, 6579–6583.
- [2] M. Sacherer, F. Hampel, H. Dube, *Nat. Commun.* **2023**, *14*, 4382.
- [3] Henrieta Volfova, Qi Hu, Eberhard Riedle, *EPA Newsletter* **2019**, 51–69.